Observational Study

Medicine®

OPEN

^{99m}Tc-3PRGD2 single-photon emission computed tomography/computed tomography for the diagnosis of choroidal melanoma

A preliminary STROBE-compliant observational study

Bing Yan, PhD[a,b], Tong Fu, MD[c,d], Yueming Liu, MD, PhD[e], Wenbin Wei, MD, PhD[e], Haojie Dai, MD[b], Wei Fang, MD, PhD[f], Feng Wang, MD, PhD[d,*]

Abstract

Recent successes in monitoring and diagnosing a variety of tumors using ^{99m}Tc-PEG4-E[PEG4-c(RGDfK)]2 (^{99m}Tc-3PRGD2) single-photon emission computed tomography (SPECT) imaging encouraged us to expand the use of this tracer. This case-control study aimed to evaluate the feasibility of ^{99m}Tc-3PRGD2 imaging for detecting choroidal melanoma (CM) and for monitoring tumor response to plaque brachytherapy (PB). Ten consecutive patients with CM who underwent ^{99m}Tc-3PRGD2 imaging before and 3 months after PB were reviewed. The tumor-to-occipital bone (T/O) and mirrored contralateral normal tissue-to-occipital bone (N/O) ratios were calculated by region of interest analysis at baseline and 3 months post-PB. T/O values were compared between patients with CM with comorbid secondary retinal detachment (RD) and those without RD. The relationship between T/O value and tumor volume was also investigated. ^{99m}Tc-3PRGD2 SPECT/CT showed focal uptake in CM. The mean T/O ratio before PB was 1.90 ± 1.26 and the mean N/O ratio was 0.80 ± 0.21 (P = .02). The ^{99m}Tc-3PRGD2 concentrations in 5 patients with CM with RD were higher (T/O = 2.69 ± 1.39) than in those without secondary RD (T/O = 1.10 ± 0.18) (P = .008). T/O ratios at 3 months post-PB were significantly lower than that at baseline (1.23 ± 0.59, P = .03). There was a linear relationship between T/O and tumor volume (y-hat = 0.028 + 0.003x, R^2 = 0.768, P = .001). The 95% confidence interval for the (T/O)/volume ratio was 0.002 to 0.005. ^{99m}Tc-3PRGD2 imaging is a feasible modality for the diagnosis of CM. Furthermore, follow-up for at least 20 months after PB indicated that coanalysis of ^{99m}Tc-3PRGD2 imaging and tumor volume may provide a promising prognostic predictor in patients with CM.

Abbreviations: 3PRGD2 = PEG4-E[PEG4-c(RGDfK)]2, FDG = ^{18}F-fluorodeoxyglucose, CDFI = color Doppler flow imaging, CI = confidence interval, CM = choroidal melanoma, COMS = collaborative ocular melanoma study, MRI = magnetic resonance imaging, N/O = normal tissue-to-occipital bone ratio, PB = plaque brachytherapy, PEG4 = 15-amino-4,7,10,13-tetraoxapentadecanoic acid, PET = positron emission tomography, RD = retinal detachment, ROI = region of interest, SPECT/CT = single-photon emission computed tomography/computed tomography, TE = time of echo, T/O = tumor-to-occipital bone ratio, TR = time of repetition.

Keywords: ^{99m}Tc-3PRGD2, angiogenesis, choroidal melanoma, integrin $\alpha_v\beta_3$

1. Introduction

Choroidal melanoma (CM) is the most common primary intraocular malignant tumor, with a high degree of malignancy.[1,2] Several therapies are available for CM, including enucleation, laser photocoagulation, photodynamic therapy, plaque radiation therapy, and external beam charged particle radiation therapy.[1,3,4] Eye-preserving surgery is the preferred option to improve the quality of life of patients with CM. The mortality rates of ^{125}I brachytherapy and enucleation are similar, and ^{125}I brachytherapy has thus been widely used and has shown great advances.[3–5] However, local treatment failure and recurrence are common after globe-conserving therapy, often necessitating further radiation or enucleation and thus increasing morbidity.[5] Traditional imaging diagnosis based on morphology showed that the combination of 3 imaging techniques [ultrasonography, magnetic resonance imaging (MRI), and fundus angiography] could diagnose CM with a sensitivity of 100% and specificity of 83.3%.[6] However, the mean tumor thickness at detection in morphological examinations is 5.0 mm,[2] indicating that the tumor was already developing or recurring, leading to delayed treatment and a poor prognosis. Diagnostic strategies focusing on tumor behaviors such as tumorigenesis and angiogenesis are therefore needed to monitor the tumor in its early stages.

Editor: Jianxun Ding.

BY and TF contributed equally to this manuscript.

Funding: This study was supported by the priming scientific research foundation for the senior researcher in Beijing TongRen Hospital, Capital Medical University (2014-YJJ-GGL-046) and the Chinese National Nature Science Foundation (81171383).

Conflict of interests: The authors have no conflicts of interest to disclose.

[a] Beijing Key Laboratory of Nasal Diseases, Beijing Institute of Otolaryngology, [b] Department of Nuclear Medicine, Beijing Tongren Hospital, Capital Medical University, Beijing, China, [c] Institute of Diagnostic and Interventional Neuroradiology, Hannover Medical School, Hannover, Germany, [d] Department of Nuclear Medicine, Nanjing First Hospital, Nanjing Medical University, Nanjing, [e] Beijing Tongren Eye Center, Beijing Tongren Hospital, Capital Medical University, [f] Cardiovascular Institute & Fu Wai Hospital, Peking Union Medical College & Chinese Academy of Medical Sciences, Beijing, China.

[*] Correspondence: Feng Wang, Department of Nuclear Medicine, Nanjing First Hospital, Nanjing Medical University, 68 Changle Road, Nanjing 210006, China (e-mail: fengwangcn@hotmail.com).

Medicine (2018) 97:40(e12441)

Received: 6 February 2018 / Accepted: 26 August 2018

http://dx.doi.org/10.1097/MD.0000000000012441

Angiogenesis is known to be crucial for the initialization, development, and metastasis of CM.[7,8] Integrin plays a fundamental role in angiogenesis and thus serves as a crucial imaging target.[9–12] The new radiolabeled tracer ^{99m}Tc-PEG4-E[PEG4-c(RGDfK)]2 (^{99m}Tc-3PRGD2) [15-amino-4,7,10,13-tetraoxapentadecanoic acid (PEG4)] targeted to integrin $\alpha_v\beta_3$, which represents an important marker of tumorigenesis and angiogenesis, has been used for the noninvasive detection of tumors and for monitoring their response to treatment. ^{99m}Tc-3PRGD2 uptake has proven safe and effective in animal cells and in patients with various cancers, including breast cancer, lung cancer, and glioma.[13–24] However, ^{99m}Tc-3PRGD2 has not been used in CM to date. The current study was designed to evaluate the efficiency of ^{99m}Tc-3PRGD2 for identifying CM and for monitoring its response to plaque brachytherapy (PB).

2. Materials and methods

2.1. Patient eligibility

This clinical study was approved by the ethics committee of Nanjing First Hospital, Nanjing Medical University. Ten consecutive patients who received a diagnosis of CM and who planned to undergo ^{125}I-PB were invited for ^{99m}Tc-3PRGD2 imaging before and 3 months post-PB. B-mode ultrasonography, color Doppler flow imaging (CDFI), and MRI were performed before PB, and B-mode ultrasonography and CDFI were also performed 3 months post-PB. The diagnosis of CM was based on fundus examination, B-mode ultrasonography, CDFI, and MRI.[1] The exclusion criteria were pregnancy and breast-feeding. Written informed consent was obtained from each patient. The study flow chart is shown in Figure 1.

2.2. MRI, B-mode ultrasonography, and CDFI examinations

Orbital MRI scans were performed using a 1.5 T MRI scanner (Signa TwinSpeed; GE Healthcare, Milwaukee, WI) with dual 7.6-mm surface coils. Spin echo T1-weighted image was carried out at a time of repetition (TR) of 600.0 ms and a time of echo (TE) of 11.1 ms. The fast spin echo T2-weighted image acquisition parameters were at TR 3000 ms and TE 120 ms. Gadopentetate dimeglumine (0.1 mmol/kg, Magnevist; Bayer Schering Pharma, Berlin, Germany) was injected and dynamic contrast-enhanced MRI were obtained employing 3D-fast spoiled gradient echo (TR 8.4 ms, TE 4.0 ms, flip angle 15°, field of view 220 × 220 mm, matrix size 256 × 160, slice thickness 3.2 mm with 0 spacing and 5 minutes acquisition time).

B-mode ultrasonography and CDFI were performed using Mylab 90× vision diagnostic instruments (Esaote, Shenzhen, China). B-type ultrasonography was used to identify the location and measure the base diameter and height of the tumor. The CM volume was calculated by the equation: $V = 2\pi a^2 b/3$, where V = tumor volume, a = base diameter/2, and b = height.[25] CDFI was used to observe tumor blood flow with a frequency range of 6 to 18 MHz.

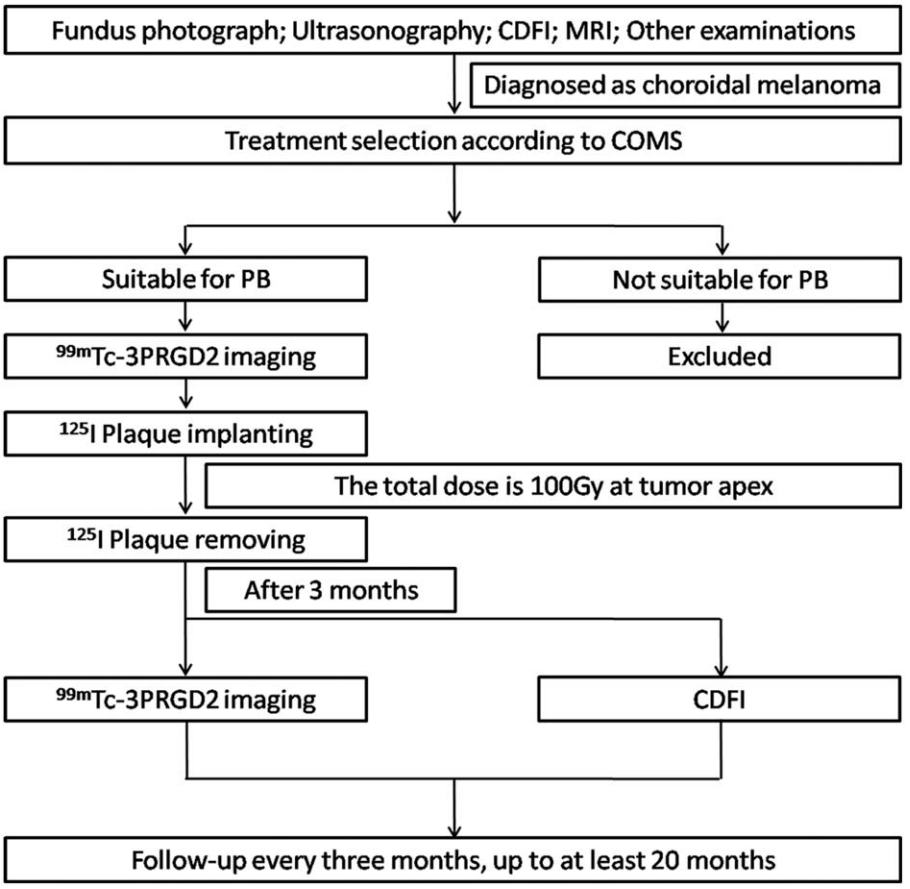

Figure 1. Study work flow. CDFI = color Doppler flow imaging, COMS = collaborative ocular melanoma study, MRI = magnetic resonance imaging, PB = plaque brachytherapy.

2.3. Radiosynthesis of ^{99m}Tc-3PRGD2

^{99m}Tc-3PRGD2 radiotracer was prepared as described previously.[18] Briefly, the kit contained 20 μg hydrazinonicotinamide-3PRGD2, 5 mg trisodium triphenylphosphine-3,3′,3″-trisulfonate, 6.5 mg tricine, 40 mg mannitol, 38.5 mg disodium succinate hexahydrate, and 12.7 mg succinic acid. For ^{99m}Tc radio labeling, 1.0 mL of 1110 to 1480 MBq (30–40 mCi) of $Na^{99m}TcO_4$ solution was added to a lyophilized vial. The vial was heated at 100°C for 20 minutes in a lead-shielded water bath and then cooled to room temperature. The resulting solution was analyzed by instant thin-layer chromatography using paper strips and acetone as eluent. The radiochemical purity was >95%.

2.4. Single-photon emission computed tomography scan

Each patient was injected with 11.1 MBq (0.3 mCi) of ^{99m}Tc-3PRGD2/kg. Head imaging was performed at rest 60 minutes after the injection of ^{99m}Tc-3PRGD2 using a dual-head SPECT/CT camera (Infinia Hawkeye IV, GE Healthcare, Fairfield, CT) equipped with a low-energy, all-purpose collimator centered on the 140-keV energy peak with a 20% symmetrical energy window. Thirty projection images were acquired over a 180° arc (0° anterior to 0° posterior position) at 6° intervals for each SPECT head. The acquisition time was 30 seconds at each projection. The transaxial data were reconstructed using Ordered Subset Expectation Maximization (2 iterations, 8 subsets). Tomographic images were displayed as coronal, sagittal, and transaxial.

2.5. SPECT imaging analysis

^{99m}Tc-3PRGD2 imaging analysis was completed by 3 experienced nuclear medicine physicians. Image quality was documented by visual analysis. For semiquantitative analysis, the tumor-to-occipital bone (T/O) and mirror contralateral normal site-to-occipital bone (N/O) radioactive ratios in the SPECT images were measured and calculated by the same person, using a consistent standard. The tumor region of interest (ROI) was drawn according to the edge of the accumulating area according to visual assessment. A mirror ROI on the contralateral eye was drawn as the normal ROI. Twelve pixels at occipital bone were drawn as occipital bone ROI. The T/O and N/O ratios were calculated as the mean counts of tumor or normal ROI/mean count of occipital bone ROI.

2.6. Statistical analysis

Statistical analysis was performed using SPSS version 23 (IBM Corp, Armonk, NY). All quantitative data were expressed as mean ± standard deviation. Differences in continuous variables were analyzed using Student *t* test, or the Mann-Whitney U test if the assumptions of a *t* test might not be met. Paired *t* tests were used to compare the T/O and N/O ratios before and after PB. Linear regression between T/O ratio and tumor volume was calculated. Statistical significance was defined as a *P* value <.05.

3. Results

3.1. Patient characteristics

Data for the 10 enrolled patients are summarized in Table 1. The patients included 5 women and 5 men, aged 25 to 78 years (mean age, 42 ± 16 years). All patients underwent B-mode ultrasound and CDFI examinations and some also received MRI scans, and all were diagnosed with CM. Five of the 10 patients were diagnosed with secondary retinal detachment (RD) by B-mode ultrasonography and/or MRI.

3.2. ^{99m}Tc-3PRGD2 imaging

The ^{99m}Tc-3PRGD2 SPECT/CT image quality was good in all 10 patients. The distribution of ^{99m}Tc-3PRGD2 in the human head could be clearly observed in coronal, sagittal, and trans-axial images (Fig. 2). In addition to intense accumulation in the lacrimal gland, nasal mucosa, and submandibular gland, which corresponded to the main excretion pathways, there was also moderate ^{99m}Tc-3PRGD2 uptake in the bone marrow. The distribution was consistent with a previous report.[20] The clear background in the eyeballs allowed easy discrimination of CM lesions.

Table 1

Clinical and imaging information for 10 patients with choroidal melanoma.

				Before PB							3rd month after PB			
				^{99m}Tc-3PRGD2		Lesion size, mm		MRI			^{99m}Tc-3PRGD2		Lesion size, mm	
No.	Sex	Age, y	RD	T/O	N/O	Base diameter	Height	T1WI	T2WI	DEC-MRI	T/O	N/O	Base diameter	Height
1	M	46	Y	2.03	1.32	14.7	5.2	Hyperintense	Hyperintense	Medium intense enhancement	1.14	0.96	13.7	3.2
2	F	27	N	1.08	0.79	12	6	–	–	–	0.79	0.57	9	4.4
3	F	25	N	1.10	0.75	11.1	6.5	Isointense	Hyperintense	Intense enhancement	0.95	0.84	11.5	5.7
4	M	32	N	0.84	0.63	12	4	Isointense	Hyperintense	Intense homogeneous enhancement	0.63	0.61	10.5	2.7
5	M	37	N	1.13	0.74	12	7	Isointense	Isointense	Intense enhancement	0.92	0.87	11.2	4.5
6 (Fig. 4)	F	55	N	1.34	0.85	9.5	3.2	–	–	–	0.97	0.79	8.6	3.2
7 (Fig. 2)	F	78	Y	5.13	0.91	14.1	13.7	Hyperintense	Hyperintense	Less intense enhancement	2.62	0.74	13	15.4
8	M	49	Y	1.78	0.69	13	9	Hyperintense	Hyperintense	Enhancement and fluid	1.32	0.78	11.2	5.2
9	F	32	Y	2.51	0.66	15.1	9.2	–	–	–	1.84	0.87	14.2	5.3
10	M	42	Y	2.02	0.61	12.6	7.2	–	–	–	1.11	0.65	14.6	6.7

– = without MRI, ^{99m}Tc-3PRGD2 = ^{99m}Tc-PEG4-E[PEG4-c(RGDfK)]2, DEC-MRI = dynamic contrast-enhanced MRI, MRI = magnetic resonance imaging, N/O = normal site-to-occipital bone ratios, No. = patient number, PB = plaque brachytherapy, RD = retinal detachment, T/O = tumor-to-occipital bone ratios, T1WI = T1-weighted image, T2WI = T2-weighted image.

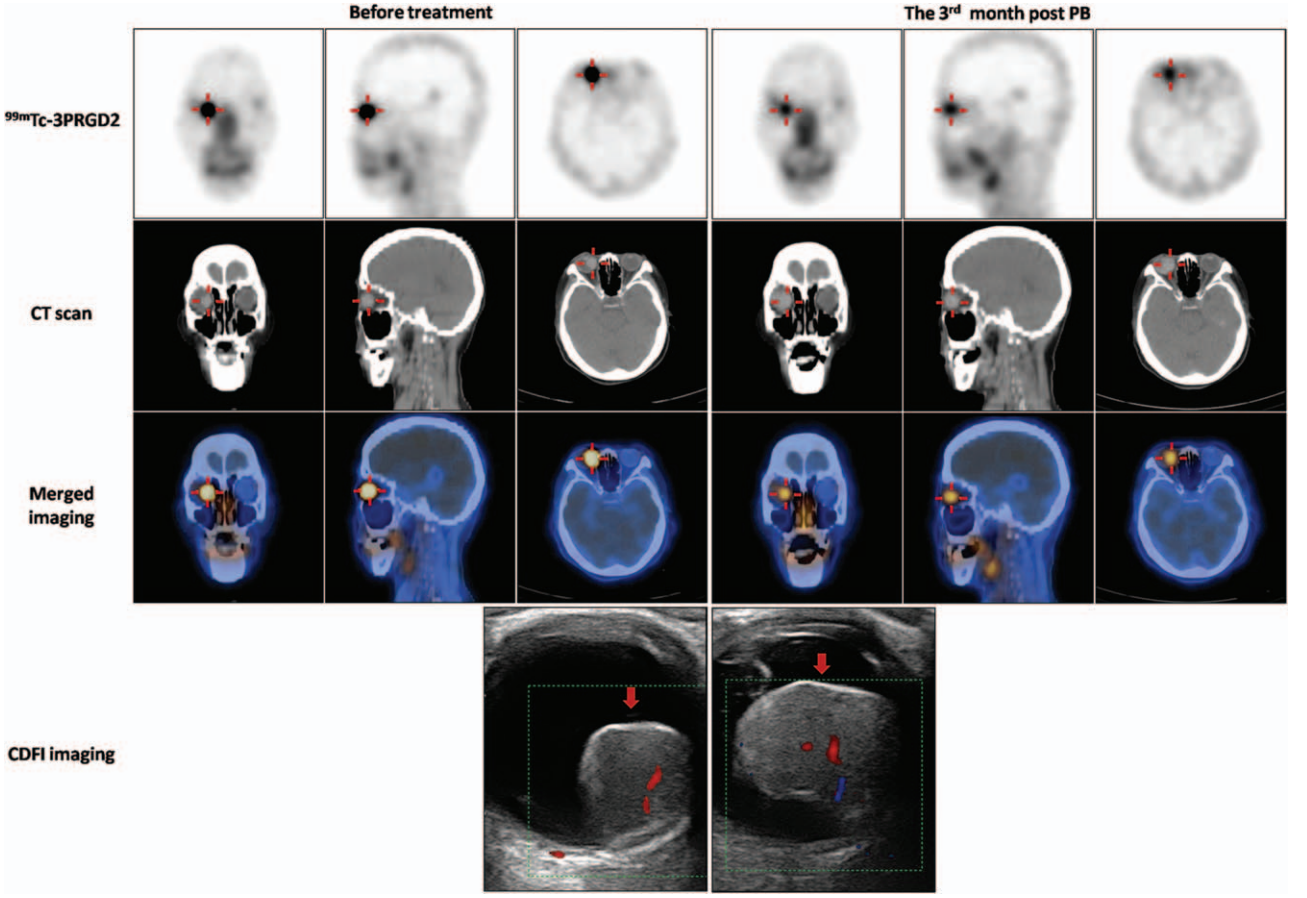

Figure 2. ^{99m}Tc-PEG4-E[PEG4-c(RGDfK)]2 (^{99m}Tc-3PRGD2) single-photon emission computed tomography/computed tomography (SPECT/CT) images (axial, sagittal, and coronal) and CDFI images before and 3 months after PB treatment in a 78-year-old woman with choroidal melanoma (CM) (patient 7). Intense accumulation of ^{99m}Tc-3PRGD2 in the lesion in the right eye (red cross) fell from tumor-to-occipital bone ratio (T/O) = 5.13, normal tissue-to-occipital bone ratio (N/O) = 0.91 before PB to T/O = 2.62, N/O = 0.74 at 3 months post-PB. B-mode ultrasonography and CDFI showed that the base length and height of the lesion varied from 14.1 and 13.7 mm, respectively (before treatment) to 13 and 15.4 mm, respectively at 3 months post-PB. CDFI = color Doppler flow imaging, CT = computed tomography, PB = plaque brachytherapy.

Imaging of patients before PB indicated that ^{99m}Tc-3PRGD2 was highly accumulated in the CM (Fig. 2). Semiquantitative analysis of the 10 patients showed a mean T/O ratio of 1.90 ± 1.26, which was significantly higher than the N/O ratio of 0.80 ± 0.21 for normal tissue (P = .02). T/O ratios had decreased in all patients at 3 months post-PB, with mean T/O and N/O ratios of 1.23 ± 0.59 and 0.77 ± 0.12, respectively (P = .03). ^{99m}Tc-3PRGD2 uptake by the CM decreased significantly after treatment (P = .02), whereas uptake by normal tissue was similar before and after treatment (P = .64) (Table 2).

The mean T/O ratio of ^{99m}Tc-3PRGD2 uptake among the 5 patients with RD before therapy was 2.69 ± 1.39, which was significantly higher than the ratio of 1.10 ± 0.18 in the 5 patients without RD (P = .008) (Table 3).

3.3. Ratio of T/O to tumor volume

Higher tumor expression of integrin $\alpha_v\beta_3$ usually indicates greater angiogenesis and metastasis. To reflect the integrin $\alpha_v\beta_3$ expression in CM patients in vivo, the ratio of T/O to volume for each patient is listed in Table 4. There was a linear relationship between T/O and volume (y-hat = 0.028 + 0.003x; R^2 = 0.768, P = .001) (Fig. 3). The 95% confidence interval (CI) for (T/O)/volume ratio before treatment was 0.002 to 0.005. The (T/O)/

Table 2

^{99m}Tc-3PRGD2 uptake and tumor volume in patients with choroidal melanoma before and 3 months after plaque brachytherapy.

	^{99m}Tc-3PRGD2 imaging			
	T/O	N/O	*P*	Volume, mm^3
Before PB	1.90 ± 1.26	0.80 ± 0.21	.02	636.00 ± 381.03
Third month after PB	1.23 ± 0.59	0.77 ± 0.12	.03	448.27 ± 373.12
P	.02	.64	–	.02

^{99m}Tc-3PRGD2 = ^{99m}Tc-PEG4-E[PEG4-c(RGDfK)]2, N/O = normal site-to-occipital bone ratios, PB = plaque brachytherapy, T/O = tumor-to-occipital bone ratios.

Table 3

^{99m}Tc-3PRGD2 uptake in patients with choroidal melanoma with or without secondary retinal detachment before and 3 months after plaque brachytherapy.

	No-RD	RD	*P*
Before PB	1.10±0.18	2.69±1.39	.008
Third month after PB	0.85±0.14	1.61±0.64	.056
P	.004	.04	–

No-RD = with no retinal detachment, PB = plaque brachytherapy, RD = retinal detachment.

volume in patient 6 was 0.0089 and was above the 95% CI. Follow-up ^{99m}Tc-3PRGD2 imaging in this patient was performed at 6 months post-PB (Fig. 4) and liver metastasis occurred at 21 months post-PB.

4. Discussion

^{18}F-fluorodeoxyglucose (FDG)-positron emission tomography (PET)/CT has been used to detect CM and to stage patients for treatment.[26–28] However, FDG has been reported to show poor concentrations in CM lesions.[29] Furthermore, ^{18}F-FDG-PET/CT imaging only reflects the metabolic situation, which represents a limitation of this technique. ^{99m}Tc-3PRGD2 is a star radiotracer for functional tumor diagnosis[13–22] and has been widely used in various kinds of tumors. We carried out the first study of ^{99m}Tc-3PRGD2 imaging in 10 patients with CM and showed that all CM lesions were positive. The mean T/O ratio was significantly higher than the mean N/O ratio, suggesting that ^{99m}Tc-3PRGD2 could be used as a sensitive detector for CM.

Table 4

Tumor-to-occipital bone ratio/tumor volume and follow-up information for each patient.

	(T/0)/V (1/mm^3)		
No	Before PB	Third month after PB	Follow-up
1	0.0035	0.0036	22nd Month, enucleation
2	0.0024	0.0042	20th Month, local control
3	0.0026	0.0024	20th Month, local control
4	0.0028	0.0040	23rd Month, local control
5	0.0021	0.0031	–
6 (Fig. 4)	0.0089	0.0078	6th Month, local recurrence; 8th Month, enucleation; 21st Month, liver metastasis
7 (Fig. 2)	0.0036	0.0019	25th Month, enucleation
8	0.0022	0.0039	–
9	0.0023	0.0033	20th Month, local control
10	0.0034	0.0015	22nd Month, local control

– = with no follow-up results, (T/O)/V = tumor-to-occipital bone ratio/tumor volume, No = patient number, PB = plaque brachytherapy.

Our results suggested that ^{99m}Tc-3PRGD2 imaging could predict melanoma progress and metastatic behavior. Because ^{99m}Tc-3PRGD2 specifically targets integrin $\alpha_v\beta_3$, which presents angiogenic activity, its decreased uptake in CM lesions 3 months after PB indicated that the therapy was effective and tumor angiogenesis had decreased. Both the Collaborative Ocular Melanoma Study (COMS) and the American Joint Commission on Cancer consider tumor size to be the most important reference

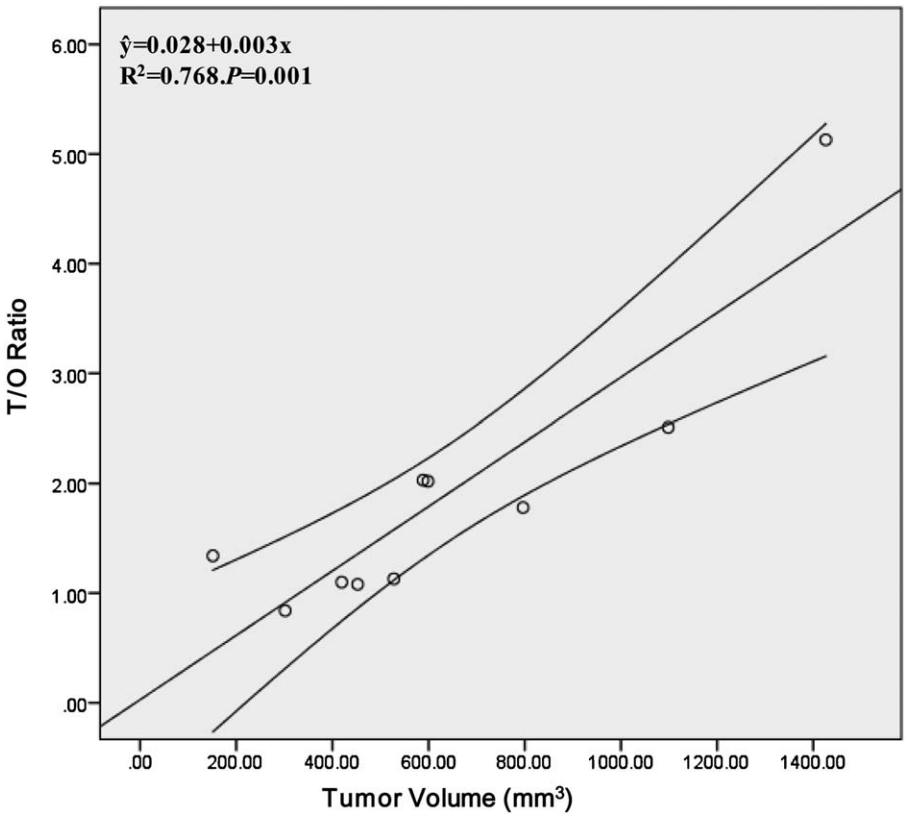

Figure 3. Linear relationship between T/O and volume. Curves represent the 95% confidence interval. T/O = tumor-to-occipital bone ratio.

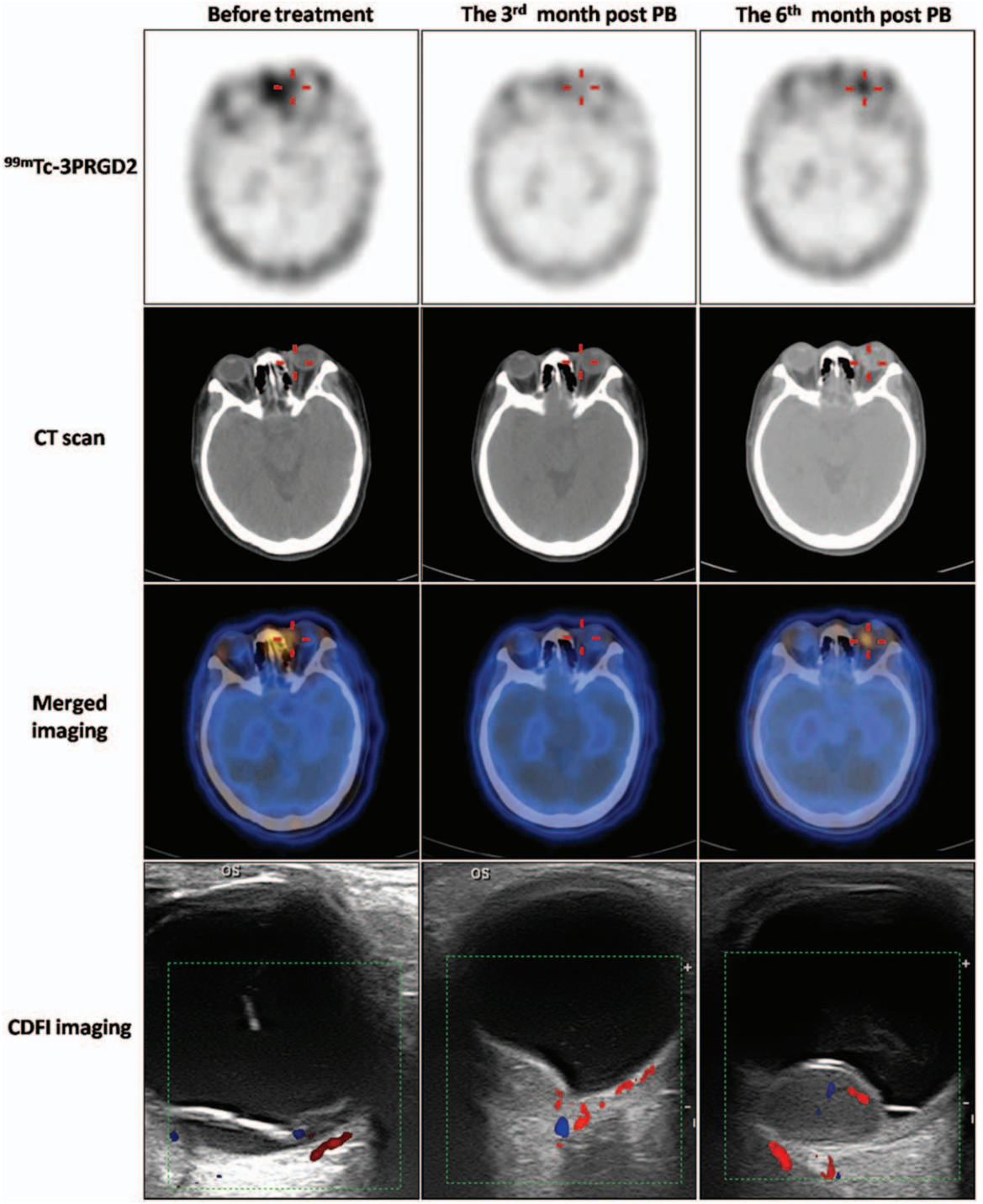

Figure 4. ^{99m}Tc-PEG4-E[PEG4-c(RGDfK)]2 (^{99m}Tc-3PRGD2) single-photon emission computed tomography/computed tomography (SPECT/CT) images (axial) and color Doppler flow imaging (CDFI) images before PB, and at 3 and 6 months post-PB treatment in a 55-year-old woman with choroidal melanoma (CM) (patient 6). Uptake of ^{99m}Tc-3PRGD2 in the lesion in the left eye (red cross) fell from tumor-to-occipital bone ratio (T/O) = 1.34 before PB to T/O = 0.97 at 3 months post-PB. Follow-up ^{99m}Tc-3PRGD2 imaging at 6 months post-PB showed increased accumulation, with T/O = 1.68. B-mode ultrasonography and CDFI showed tumor sizes of 9.5 × 3.2, 8.6 × 3.2, and 14.3 × 9.1 mm before treatment and at 3 and 6 months post-PB, respectively. Enucleation was done at 8 months after PB. Unfortunately, liver metastasis was detected at about 21 months post-PB. However, this information was acquired by phone interview and no liver metastasis images were available because the patient was not a resident of Peking. CDFI = color Doppler flow imaging, CT = computed tomography, PB = plaque brachytherapy.

for classifying CM and for choosing the most appropriate treatment.[3,4] However, tumor size alone may not be the best index, because locally shrunk tumors can also be associated with distant metastasis. Furthermore, delayed recurrence and metastasis still occur in medium-sized and T2 to T4-stage tumors.[5] Patients with disease-free survival or better following treatment for primary uveal melanoma may still develop remote metastasis. One hypothesis suggested that angiogenesis may cause cancer

latency, leading to delayed recurrence and remote metastasis.[4] One of our patients (patient 6) received PB therapy according to COMS, and the tumor had decreased to medium size 3 months later. No further therapy was administered in accordance with COMS guidelines. However, ^{99m}Tc-3PRGD2 accumulation increased, suggesting that the tumor was in an invasive state, and liver metastasis was accordingly detected at 21 months post-PB. This supports the idea that angiogenesis is closely related to the progress of CM. Tumor size and ^{99m}Tc-3PRGD2 uptake combined was used to predict the prognosis of CM in this study. According to the linear regression, tracer accumulation was correlated with tumor size, that is, bigger tumors showed higher levels of integrin$\alpha_v\beta_3$ expression. However, once the (T/O)/volume ratio exceeded the 95% CI, the increase in integrin $\alpha_v\beta_3$ expression no longer matched tumor volume. Patient 6 showed no tumor enlargement and no RD, but a high (T/O)/volume ratio pre- and post-PB treatment, both of which were above the 95% CI (0.002–0.005). This patient experienced recurrence of CM at 6 months post-PB, and liver metastasis at 21 months post-PB. This may suggest that the reverse high uptakes of ^{99m}Tc-3PRGD2 to the shrink or stable tumor size indicated high activity of angiogenesis, leading to high risk of metastasis. It also suggests that (T/O)/volume may provide a promising index for assessing tumor development and metastasis risk. (T/O)/volume in patients with CM may play a more predominant role in predicting tumor progress than T/O or volume alone, and a small tumor with a high T/O may thus have a poor prognosis. Long-term ^{99m}Tc-3PRGD2 imaging should thus be performed to allow clinicians to judge the possibility of recurrence and metastasis and to take the appropriate actions.

Brachytherapy is widely used according to COMS to preserve visual acuity and improve the patient's quality of life.[3] However, various radiation-related complications may occur, such as optic neuropathy, maculopathy, cataract, neovascular glaucoma, ischemia, RD, and vessel obstruction, and thus decreasing quality of life.[30] Adjuvant treatments can be used to help prevent and treat these complications. Meanwhile, antiangiogenesis therapy involving antivascular endothelial growth factor therapy, anti-integrin $\alpha_v\beta_3$ therapy, Arg-Gly-Asp (RGD) peptides-related chemotherapy, and gene therapy have all demonstrated progress.[31–34]^{99m}Tc-3PRGD2 reflects the integrin $\alpha_v\beta_3$ expression level in vivo and provides a noninvasive assessment of angiogenesis, and thus supporting the use and monitoring of angiogenesis-related adjuvant therapies.

There were several limitations in this study. First, ROI was drawn by visual analysis; thus, the data may have some bias. Kinds of means were adopted to minimize this influence: the T/O and N/O ratios were measured by the same person using a consistent standard. The tumor ROI was drawn by the edge of accumulating area and a mirror ROI on the contralateral eye was drawn as normal ROI. We also draw the fixed 12 pixels at occipital bone as occipital bone ROI to minimize the difference of absorption resulting from ROI area difference. Second, the number of enrolled patients was inadequate. This study showed only the preliminary result of the uptake of ^{99m}Tc-3PRGD2 in CM. We observed one case that for which, the ratio of (T/O)/V was above the 95% CI at the baseline and liver metastasis happened at 21st-month post-PB. Cohorts and follow-up studies with more patients will be needed to confirm this finding and to investigate the role of ^{99m}Tc-3PRGD2 imaging in the prediction of metastasis.

In conclusion, ^{99m}Tc-3PRGD2 may be an effective diagnostic tool in patients with CM, with promising potential for monitoring the response to therapy and for predicting prognosis.

Acknowledgments

The authors thank Wu Lijuan, from Department of Epidemiology and Biostatistics, Capital Medical University, for providing statistical consultation. The authors also thank Susan Furness, PhD, from Liwen Bianji, Edanz Group China (www.liwenbianji.cn/ac), for editing the English text of a draft of this manuscript.

Author contributions

Bing Yan and Tong Fu contributed to most of the study design, data analysis, and manuscript drafting; Yueming Liu and Wenbin Wei helped to enroll the patients and to revise the manuscript; Haojie Dai, Wei Fang, and Feng Wang analyzed the imaging; and Feng Wang designed the study, revised the manuscript, and acquired the grant support.

Data curation: Bing Yan.
Formal analysis: Bing Yan, Tong Fu.
Investigation: Bing Yan.
Methodology: Bing Yan, Tong Fu, Wenbin Wei.
Project administration: Yueming Liu.
Supervision: Haojie Dai.
Visualization: Wei Fang.
Writing – original draft: Bing Yan, Tong Fu.
Writing – review and editing: Feng Wang.

References

[1] Singh P, Singh A. Choroidal melanoma. Oman J Ophthalmol 2012;5:3–9.
[2] Shields CL, Manalac J, Das C, et al. Choroidal melanoma: clinical features, classification, and top 10 pseudomelanomas. Curr Opin Ophthalmol 2014;25:177–85.
[3] Collaborative Ocular Melanoma Study GroupThe COMS randomized trial of iodine 125 brachytherapy for choroidal melanoma: V. Twelve-year mortality rates and prognostic factors: COMS rep-ort No. 28. Arch Ophthalmol 2006;124:1684–93.
[4] American Brachytherapy Society—Ophthalmic Oncology Task Force, ABS—OOTF CommitteeThe American Brachytherapy Society consensus guidelines for plaque brachytherapy of uveal melanoma and retinoblastoma. Brachytherapy 2014;13:1–4.
[5] Chang MY, McCannel TA. Local treatment failure after globe-conserving therapy for choroidal melanoma. Br J Ophthalmol 2013;97:804–11.
[6] Yan B, Qiu F, Ren L, et al. 99mTc-3P-RGD2 molecular imaging targeting integrin alphavbeta3 in head and neck squamous cancer xenograft. J Radioanal Nucl Chem 2015;304:1171–7.
[7] Tapper D, Langer R, Bellows AR, et al. Angiogenesis capacity as a diagnostic marker for human eye tumors. Surgery 1979;86:36–40.
[8] Xu Q, Zhao GQ, Zhao J, et al. Expression and significance of factors related to angiogenesis in choroidal melanoma. Int J Ophthalmol 2011;4:49–54.
[9] Foubert P, Varner JA. Integrins in tumor angiogenesis and lymphangiogenesis. Methods Mol Biol 2012;757:471–86.
[10] Demircioglu F, Hodivala-Dilke K. alphavbeta3 Integrin and tumour blood vessels-learning from the past to shape the future. Curr Opin Cell Biol 2016;42:121–7.
[11] Danhier F, Le Breton A, Préat V. RGD-based strategies to target alpha(v) beta(3) integrin in cancer therapy and diagnosis. Mol Pharm 2012;9:2961–73.
[12] Gaertner FC, Kessler H, Wester HJ, et al. Radiolabelled RGD peptides for imaging and therapy. Eur J Nucl Med Mol Imaging 2012;39(suppl 1):S126–38.
[13] Liu Z, Wang F. Development of RGD-based radiotracers for tumor imaging and therapy: translating from bench to bedside. Curr Mol Med 2013;13:1487–505.
[14] Zhou Y, Kim YS, Chakraborty S, et al. 99mTc-labeled cyclic RGD peptides for noninvasive monitoring of tumor integrin alphaVbeta3 expression. Mol Imaging 2011;10:386–97.
[15] Ma Q, Ji B, Jia B, et al. Differential diagnosis of solitary pulmonary nodules using (9)(9)mTc-3P(4)-RGD(2) scintigraphy. Eur J Nucl Med Mol Imaging 2011;38:2145–52.

[16] Jia B, Liu Z, Zhu Z, et al. Blood clearance kinetics, biodistribution, and radiation dosimetry of a kit-formulated integrin alphavbeta3-selective radiotracer 99mTc-3PRGD 2 in non-human primates. Mol Imaging Biol 2011;13:730–6.
[17] Zhao D, Jin X, Li F, et al. Integrin alphavbeta3 imaging of radioactive iodine-refractory thyroid cancer using 99mTc-3PRGD2. J Nucl Med 2012;53:1872–7.
[18] Fu T, Qu W, Qiu F, et al. (99m)Tc-3P-RGD2 micro-single-photon emission computed tomography/computed tomography provides a rational basis for integrin alphavbeta3-targeted therapy. Cancer Biother Radiopharm 2014;29:351–8.
[19] Chakravarty R, Chakraborty S, Dash A. Molecular Imaging of Breast Cancer: Role of RGD Peptides. Mini Rev Med Chem 2015;15:1073–94.
[20] Zhu Z, Miao W, Li Q, et al. 99mTc-3PRGD2 for integrin receptor imaging of lung cancer: a multicenter study. J Nucl Med 2012;53: 716–22.
[21] Ji S, Zhou Y, Voorbach MJ, et al. Monitoring tumor response to linifanib therapy with SPECT/CT using the integrin alphavbeta3-targeted radiotracer 99mTc-3P-RGD2. J Pharmacol Exp Ther 2013;346:251–8.
[22] Shao G, Zhou Y, Wang F, et al. Monitoring glioma growth and tumor necrosis with the U-SPECT-II/CT scanner by targeting integrin alphavbeta3. Mol Imaging 2013;12:39–48.
[23] Zhao ZQ, Yang Y, Fang W, et al. Comparison of biological properties of 99mTc-labeled cyclic RGD Peptide trimer and dimer useful as SPECT radiotracers for tumor imaging. Nucl Med Biol 2016;43:661–9.
[24] Xu D, Zhao ZQ, Chen ST, et al. Iminodiacetic acid as bifunctional linker for dimerization of cyclic RGD peptides. Nucl Med Biol 2017;48:1–8.
[25] Richtig E, Langmann G, Mullner K, et al. Calculated tumour volume as a prognostic parameter for survival in choroidal melanomas. Eye (Lond) 2004;18:619–23.
[26] Freton A, Chin KJ, Raut R, et al. Initial PET/CT staging for choroidal melanoma: AJCC correlation and second nonocular primaries in 333 patients. Eur J Ophthalmol 2012;22:236–43.
[27] Mena E, Taghipour M, Sheikhbahaei S, et al. 18F-FDG PET/CT and melanoma: value of fourth and subsequent posttherapy follow-up scans for patient management. Clin Nucl Med 2016;41:e403–9.
[28] Matsuo T, Ogino Y, Ichimura K, et al. Clinicopathological correlation for the role of fluorodeoxyglucose positron emission tomography computed tomography in detection of choroidal malignant melanoma. Int J Clin Oncol 2014;19:230–9.
[29] Sharma RS, Shah PK, Narendran V. Poor uptake of fluorodeoxyglucose in positron emission tomography-computed tomography scan for intraocular choroidal melanoma in Asian Indian eyes. World J Nucl Med 2016;15:53–5.
[30] Pereira PR, Odashiro AN, Lim LA, et al. Current and emerging treatment options for uveal melanoma. Clin Ophthalmol 2013;7:1669–82.
[31] Weis SM, Cheresh DA. Tumor angiogenesis: molecular pathways and therapeutic targets. Nat Med 2011;17:1359–70.
[32] Vachutinsky Y, Oba M, Miyata K, et al. Antiangiogenic gene therapy of experimental pancreatic tumor by sFlt-1 plasmid DNA carried by RGD-modified crosslinked polyplex micelles. J Control Release 2011;149:51–7.
[33] Shojaei F. Anti-angiogenesis therapy in cancer: current challenges and future perspectives. Cancer Lett 2012;320:130–7.
[34] Rubtsov MA, Syrkina MS, Aliev G. RGD-based therapy: principles of selectivity. Curr Pharm Des 2016;22:932–52.